On The Minimum-Time Reorientation of a Rigid Body

Andrew Fleming*

Leffler Consulting LLC, Chantilly, VA, 20152, USA.

Pooya Sekhavat† and I. Michael Ross‡

Naval Postgraduate School, Monterey, CA, 93943, USA

Recent advances in optimal control theory and computation are used to develop minimum-time solutions for the rest-to-rest reorientation of a generic rigid-body. It is shown that the differences in the geometry of the inertia ellipsoid and the control space lead to counter-intuitive non-eigenaxis maneuvers. The optimality of the open-loop solutions are verified by an application of Pontryagin's Principle as a necessary condition and not as a problem-solving tool. It is shown that the nonsmoothness of the lower Hamiltonian compounds the curse of dimensionality associated in solving the Hamilton-Jacobi-Bellman equations for feedback solutions. These difficulties are circumvented by generating Carathéodory-π trajectories which are based on the fundamental notion that closed-loop does not necessarily imply closed-form solutions. While demonstrating the successful implementation of the proposed method for practical applications, these closed-loop results reveal yet another counter-intuitive phenomenon: a suggestion that parameter uncertainties may aid the optimality of the maneuver rather than hinder it.

I. Introduction

In their pioneering work[1] of 1993, Bilimoria and Wie closed the door on the eigenaxis maneuver as the minimum-time solution to the reorientation of a rigid body. By considering the minimum-time problem for the simple tri-axisymmetric (cubical or spherical) rigid body they reduced the issues to the core principles of why eigenaxis maneuvering was not optimal. Despite their convincing results and obvious applications to spacecraft and robotic systems, generating time-optimal solutions to generic (i.e. asymmetric) rigid bodies remained an open problem for a long time.

In 1999, Shen and Tsiotras[2] addressed the problem of reorientating the symmetry axis of an axisymmetric rigid body. They were able to advance the work of Bilimoria and Wie from a tri-axisymmetric body to an axisymmetric body by utilizing a unique kinematic parameterization[3] and assuming an underactuated spacecraft; i.e. a body with only two control torques. They noted a major difficulty with their methodology was developing initial guesses for the costates which do not, in general, have intuitive physical interpretation. Despite these difficulties and limitations, the results of Shen and Tsiotras have practical applications as many more spacecraft can be approximated as axisymmetric than tri-axisymmetric. Because asymmetric rigid bodies are more commonplace, Proulx and Ross[4] addressed this generic problem in 2001. They used the then-new Legendre pseudospectral (PS) method[5,6] to solve the problem and overcame some of the previous numerical difficulties. Due to the limitations of the early PS methods, they developed an algorithm that combined genetic search methods with PS methods. Optimality was once again verified through compliance with Pontryagin's Principle; however, this time, Pontryagin's Principle was was not directly used as a computational technique, rather, the Covector Mapping Theorem of Ross and Fahroo[7,8] was employed to use Pontryagin's Principle as a necessary condition. Advances in PS methods allowed Fleming et al[9,10] to overcome much of the prior numerical difficulties to present results for the general case of an asymmetric rigid body, including the case for a fully-actuated axisymmetric spacecraft.[9,11]

---

*Research Scientist, Aerospace Engineering, Leffler Consulting LLC, Chantilly, VA, 20152, USA. AIAA Senior Member.
†Research Scientist, Mechanical and Astronautical Engineering, NPS. AIAA Member.
‡Professor, Mechanical and Astronautical Engineering, NPS. AIAA Associate Fellow.

American Institute of Aeronautics and Astronautics

The unifying theme of all these works is that the minimum-time reorientation problem presents unique challenges that have held the interest of engineers for over 15 years. Recent results in optimal control theory[12,13] indicate that solving the open-loop problem within the generalized time-constant of the system (roughly the inverse of the Lipschitz constant of the dynamics) is the key to optimal feedback control in the sense of generating Carathéodory-π trajectories;[12–15] please see the Appendix I for an introduction to this concept. This implies that a central problem in slew maneuvering is the reliable generation of time-optimal open-loop solutions. Consequently, we begin by examining the time-optimal reorientation of a rigid asymmetric body under the influence of three independent torques. This problem is important in its own right as it benchmarks other slew maneuvers while holding the potential as a possible feedforward controller in a two-degree-of-freedom control system architecture. In any event, we verify the optimality of the open-loop solutions by an application of Pontryagin's Principle. A direct application of Bellman's Principle is used as a companion verification principle in the sense of a necessary condition for optimality. Having verified optimality principles, we address the problem of generating closed-loop optimal controls. Carathéodory-π trajectories are generated using established, flight-proven PS techniques[12,16–18] that are also widely available through well-known software packages.[19,20] While demonstrating the successful implementation of the proposed method for practical applications, a careful selection of parameter uncertainties are introduced to reveal an apparently counter-intuitive phenomenon: a suggestion that parameter uncertainties may aid the optimality of the maneuver rather than hinder it.

II.   Problem Formulation

Let the state of the rigid body be represented by,

$$\mathbf{x} = \begin{bmatrix} \mathbf{q} \\ \boldsymbol{\omega} \end{bmatrix} \in \mathbb{R}^7 \tag{1}$$

where $\mathbf{q}$ and $\boldsymbol{\omega}$ are the familiar quaternions and body rates. Then, the state dynamics in assumed inertial space are given by the well-known dynamics,[21]

$$
\begin{aligned}
\dot{q}_1 &= \frac{1}{2} \left[\omega_1 q_4 - \omega_2 q_3 + \omega_3 q_2 \right] \\
\dot{q}_2 &= \frac{1}{2} \left[\omega_1 q_3 + \omega_2 q_4 - \omega_3 q_1 \right] \\
\dot{q}_3 &= \frac{1}{2} \left[-\omega_1 q_2 + \omega_2 q_1 + \omega_3 q_4 \right] \\
\dot{q}_4 &= \frac{1}{2} \left[-\omega_1 q_1 - \omega_2 q_2 - \omega_3 q_3 \right] \\
\dot{\omega}_1 &= \frac{u_1}{I_1} - \left(\frac{I_3 - I_2}{I_1} \right) \omega_2 \omega_3 \\
\dot{\omega}_2 &= \frac{u_2}{I_2} - \left(\frac{I_1 - I_3}{I_2} \right) \omega_1 \omega_3 \\
\dot{\omega}_3 &= \frac{u_3}{I_3} - \left(\frac{I_1 - I_2}{I_3} \right) \omega_1 \omega_2
\end{aligned}
\tag{2}
$$

The state and control spaces for the problem are given by,

$$\mathbb{X} \quad := \quad \{ \mathbf{x} \in \mathbb{R}^7 : \| \mathbf{q} \|_2 = 1 \} \tag{3}$$
$$\mathbb{U} \quad := \quad \{ \mathbf{u} \in \mathbb{R}^3 : \| \mathbf{u} \|_\infty \le u_{max} \} \tag{4}$$

The optimal control problem is to find the state-control function pair, $t \to (\mathbf{x}, \mathbf{u}) \in \mathbb{X} \times \mathbb{U}$, that will drive the spacecraft from its initial position, $\mathbf{x}(t_0) = \mathbf{x}_0$ to its final position given by $\mathbf{x}(t_f) = \mathbf{x}_f$ while minimizing the cost function,

$$J \left[\mathbf{x} \left(\cdot \right), \mathbf{u} \left(\cdot \right), t_f \right] = t_f - t_0 \tag{5}$$

For the purposes of representative analysis, we use the parameters provided in Table 1. In the same spirit,

Table 1. Data for the generic rigid body adopted from NASA's XTE Spacecraft

Parameter	Value	Units
I_1	5621	$Kg * m^2$
I_2	4547	$Kg * m^2$
I_3	2364	$Kg * m^2$

we consider the representative boundary conditions given by,

$$\begin{aligned} \mathbf{x}_0 &= [0,0,0,1,0,0,0]^T \\ \mathbf{x}_f &= \left[\frac{\sin(\phi)}{2},0,0,\frac{\cos(\phi)}{2},0,0,0\right]^T \end{aligned} \tag{6}$$

where, ϕ is the eigenaxis rotation angle.

III. Optimality Conditions

The control Hamiltonian[15, 22] for the generic spacecraft is given by,

$$\begin{aligned} H\left(\boldsymbol{\lambda}, \mathbf{x}, \mathbf{u}\right) = &\frac{\boldsymbol{\lambda}_{q_1}}{2}\left(\omega_1 q_4 - \omega_2 q_3 + \omega_3 q_2\right) + \frac{\boldsymbol{\lambda}_{q_2}}{2}\left(\omega_1 q_3 + \omega_2 q_4 - \omega_3 q_1\right) + \\ &\frac{\boldsymbol{\lambda}_{q_3}}{2}\left(-\omega_1 q_2 + \omega_2 q_1 + \omega_3 q_4\right) + \frac{\boldsymbol{\lambda}_{q_4}}{2}\left(-\omega_1 q_1 - \omega_2 q_2 - \omega_3 q_3\right) + \\ &\boldsymbol{\lambda}_{\omega 1}\left(\frac{u_1}{I_1} - \left(\frac{I_3 - I_2}{I_1}\right)\omega_2\omega_3\right) + \boldsymbol{\lambda}_{\omega 2}\left(\frac{u_2}{I_2} - \left(\frac{I_1 - I_3}{I_2}\right)\omega_1\omega_3\right) + \\ &\boldsymbol{\lambda}_{\omega 3}\left(\frac{u_3}{I_3} - \left(\frac{I_1 - I_2}{I_3}\right)\omega_1\omega_2\right) \end{aligned} \tag{7}$$

where $\boldsymbol{\lambda}$ with the appropriate subscripts denotes some generalized gradient of a verification function, $\varphi(\mathbf{x}, t)$, in the case of sufficiency conditions.[15] Deferring, for the moment, the case of necessary conditions, the lower Hamiltonian[15, 22] is given by,

$$\mathcal{H}(\boldsymbol{\lambda}, \mathbf{x}) := \min_{\mathbf{u} \in \mathbb{U}} H(\boldsymbol{\lambda}, \mathbf{x}, \mathbf{u}) \tag{8}$$

In order to solve the nonlinear programming problem given by the right hand side of 8, we apply the standard Karush-Kuhn-Tucker (KKT) theorems.[23] Thus, from the gradient normality condition of the KKT theorem, we have,

$$\begin{aligned} \frac{\boldsymbol{\lambda}_{\omega_1}}{I_1} + \mu_1 &= 0 \\ \frac{\boldsymbol{\lambda}_{\omega_2}}{I_2} + \mu_2 &= 0 \\ \frac{\boldsymbol{\lambda}_{\omega_3}}{I_3} + \mu_3 &= 0 \end{aligned} \tag{9}$$

where $\mu_i \quad i = 1, 2, 3$ are the KKT multipliers[23] associated with the Hamiltonian Minimization Condition. These KKT multipliers satisfy the complementary conditions,

$$\mu_i \begin{cases} \leq 0 & \text{if } u_i = -u_{max} \\ \geq 0 & \text{if } u_i = u_{max} \\ = 0 & \text{if } -u_{max} \leq u_i \leq u_{max} \end{cases} \tag{10}$$

We now utilize some of the modern connections between the KKT conditions and nonsmooth calculus.[15, 22] In nonsmooth calculus, a multifunction is a set-valued map; that is, while a function is a point-to-point map,
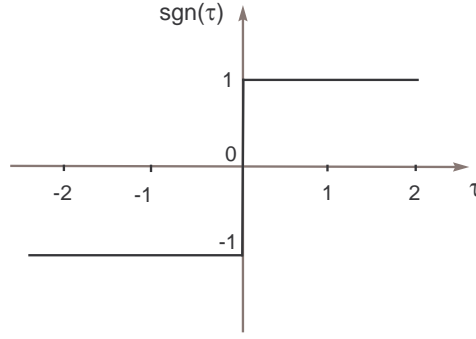
Figure 1. Graph of the sgn multifunction illustrating its multi-valued nature at $\tau = 0$.

a multifunction is a point-to-set map. A sgn multifunction (see Fig. 1) is a generalization of a sgn function defined as,

$$sgn(\tau) = \begin{cases} -1 & \tau \leq 0 \\ [-1, \ 1] & \tau = 0 \\ 1 & \tau \geq 0 \end{cases} \tag{11}$$

Thus, in nonsmooth analysis, $sgn(\tau)$ is the set $[-1, 1]$ at $\tau = 0$. This concept conforms to the engineering notion of how a sgn function is visualized as illustrated in figure 1. Thus, the difficulties of how to define a a sgn function at $\tau = 0$ are eliminated in a single stroke; however, the price we pay for this nicety is the modern concept of nonsmooth calculus.[15]

The sgn multifunction allows us to write the KKT complementarity condition, 10, in closed form,

$$u_i = u_{max} sgn(\mu_i) \tag{12}$$

Thus, the control is set-valued and a nonsmooth function of μ_i. This point illustrates a well-known fact in nonsmooth analysis[15,22] that even though the problem data in an optimal control problem may be smooth, many of the functions required for analysis, including the optimal control itself may be nonsmooth. Thus, nonsmooth analysis is not limited to problems with nonsmooth data; rather, it is quite essential even for the analysis of smooth problems. In any event, using the gradient normality condition, 9, we can eliminate the KKT multiplier from 12 to yield,

$$u_i = u_{max} sgn(-\lambda_{\omega_i}/I_i) \tag{13}$$

Substituting 13 in 7 provides an expression for the lower Hamiltonian,

$$\begin{aligned} \mathcal{H}\left(\boldsymbol{\lambda}, \mathbf{x}\right) = {} & \frac{\boldsymbol{\lambda}_{q_1}}{2}\left(\omega_1 q_4 - \omega_2 q_3 + \omega_3 q_2\right) + \frac{\boldsymbol{\lambda}_{q_2}}{2}\left(\omega_1 q_3 + \omega_2 q_4 - \omega_3 q_1\right) + \\ & \frac{\boldsymbol{\lambda}_{q_3}}{2}\left(-\omega_1 q_2 + \omega_2 q_1 + \omega_3 q_4\right) + \frac{\boldsymbol{\lambda}_{q_4}}{2}\left(-\omega_1 q_1 - \omega_2 q_2 - \omega_3 q_3\right) + \\ & \boldsymbol{\lambda}_{\omega 1}\left(\frac{u_{max} sgn(-\lambda_{\omega_1}/I_1)}{I_1} - \left(\frac{I_3 - I_2}{I_1}\right)\omega_2\omega_3\right) + \boldsymbol{\lambda}_{\omega 2}\left(\frac{u_{max} sgn(-\lambda_{\omega_2}/I_2)}{I_2} - \left(\frac{I_1 - I_3}{I_2}\right)\omega_1\omega_3\right) + \\ & \boldsymbol{\lambda}_{\omega 3}\left(\frac{u_{max} sgn(-\lambda_{\omega_3}/I_3)}{I_3} - \left(\frac{I_1 - I_2}{I_3}\right)\omega_1\omega_2\right) \end{aligned} \tag{14}$$

Note that the lower Hamiltonian is nonsmooth in $\boldsymbol{\lambda}$; hence, $\mathcal{H}(\boldsymbol{\lambda}, \mathbf{x})$ cannot be differentiated using ordinary calculus concepts. In sharp contrast, the control Hamiltonian is smooth; see 7. Because the lower Hamiltonian is nonsmooth, the Hamilton-Jacobi-Bellman (HJB) equation,

$$\mathcal{H}(\partial_{\mathbf{x}}\varphi(\mathbf{x}, t), \mathbf{x}) + \partial_t\varphi(\mathbf{x}, t) = 0 \tag{15}$$

cannot even be written within the realm of ordinary smooth calculus. This is one of the primary reasons why finding optimal feedback solutions to the time-optimal rigid body problem have long been considered difficult, if not impossible. Advances in optimal control theory over the last two decades have shown that if

American Institute of Aeronautics and Astronautics

we replace the notion of $\partial_{\mathbf{x}}\varphi(\mathbf{x}, t)$ and $\partial_t\varphi(\mathbf{x}, t)$ with the concept of the proximal subdifferential[15,22] denoted by $\partial_{\mathbf{x}}^P\varphi(\mathbf{x}, t)$ and $\partial_t^P\varphi(\mathbf{x}, t)$ respectively, then, the HJB equation can be written as a proximal HJB equation,

$$\frac{\partial_{q_1}^P\varphi(\mathbf{x}, t)}{2}(\omega_1 q_4 - \omega_2 q_3 + \omega_3 q_2) + \frac{\partial_{q_2}^P\varphi(\mathbf{x}, t)}{2}(\omega_1 q_3 + \omega_2 q_4 - \omega_3 q_1) +$$

$$\frac{\partial_{q_3}^P\varphi(\mathbf{x}, t)}{2}(-\omega_1 q_2 + \omega_2 q_1 + \omega_3 q_4) + \frac{\partial_{q_4}^P\varphi(\mathbf{x}, t)}{2}(-\omega_1 q_1 - \omega_2 q_2 - \omega_3 q_3) +$$

$$\partial_{\omega_1}^P\varphi(\mathbf{x}, t)\left(\frac{u_{max}sgn(\partial_{\omega_1}^P\varphi(\mathbf{x}, t)/I_1)}{I_1} - \left(\frac{I_3 - I_2}{I_1}\right)\omega_2\omega_3\right)$$

$$+\partial_{\omega_2}^P\varphi(\mathbf{x}, t)\left(\frac{u_{max}sgn(\partial_{\omega_2}^P\varphi(\mathbf{x}, t)/I_2)}{I_2} - \left(\frac{I_1 - I_3}{I_2}\right)\omega_1\omega_3\right) +$$

$$\partial_{\omega_3}^P\varphi(\mathbf{x}, t)\left(\frac{u_{max}sgn(\partial_{\omega_3}^P\varphi(\mathbf{x}, t)/I_3)}{I_3} - \left(\frac{I_1 - I_2}{I_3}\right)\omega_1\omega_2\right) + \partial_t^P\varphi(\mathbf{x}, t) = 0 \qquad (16)$$

This equation does have a solution; however, $\varphi(\mathbf{x}, t)$ is merely continuous. Despite recent advances[24,25] in Max-Plus algebra that eliminate the curse of dimensionality associated with the HJB equation, it is clear that finding a solution to 16 remains a formidable task. If one can find $\varphi(\mathbf{x}, t)$, then the optimal feedback controller is a consequence of 13 and given by,

$$u_i \equiv u_i(\mathbf{x}, t) := u_{max}sgn(\partial_{\omega_i}^P\varphi(\mathbf{x}, t)/I_i) \qquad (17)$$

It is possible to obtain an optimal feedback controller via a different route.[12] In this approach, we regard $\boldsymbol{\lambda}$ as an adjoint covector; then, the necessary conditions for optimality follow from Pontryagin's Principle. In this situation, the optimal control is still a consequence of 13; however, it is initially given in an open-loop construct by,

$$u_i \equiv u_i(t) = u_{max}sgn(\lambda_{\omega_i}(t)/I_i) \qquad (18)$$

where $\boldsymbol{\lambda}$ is given by the adjoint equations,

$$\begin{aligned}
\dot{\lambda}_{q_1} &= \frac{1}{2}(\lambda_{q_2}\omega_3 - \lambda_{q_3}\omega_2 + \lambda_{q_4}\omega_1) \\
\dot{\lambda}_{q_2} &= \frac{1}{2}(-\lambda_{q_1}\omega_3 + \lambda_{q_3}\omega_1 + \lambda_{q_4}\omega_2) \\
\dot{\lambda}_{q_3} &= \frac{1}{2}(\lambda_{q_1}\omega_2 - \lambda_{q_2}\omega_1 + \lambda_{q_4}\omega_3) \\
\dot{\lambda}_{q_4} &= \frac{1}{2}(-\lambda_{q_1}\omega_1 - \lambda_{q_2}\omega_2 - \lambda_{q_3}\omega_3) \\
\dot{\lambda}_{\omega_1} &= \frac{1}{2}(-\lambda_{q_1}q_4 - \lambda_{q_2}q_3 + \lambda_{q_3}q_2 + \lambda_{q_4}q_1) + \lambda_{\omega_2}\left(\frac{I_1 - I_3}{I_2}\right)\omega_3 + \lambda_{\omega_3}\left(\frac{I_2 - I_1}{I_3}\right)\omega_2 \\
\dot{\lambda}_{\omega_2} &= \frac{1}{2}(\lambda_{q_1}q_3 - \lambda_{q_2}q_4 - \lambda_{q_3}q_1 + \lambda_{q_4}q_2) + \lambda_{\omega_1}\left(\frac{I_3 - I_2}{I_1}\right)\omega_3 + \lambda_{\omega_3}\left(\frac{I_2 - I_1}{I_3}\right)\omega_1 \\
\dot{\lambda}_{\omega_3} &= \frac{1}{2}(-\lambda_{q_1}q_2 + \lambda_{q_2}q_1 - \lambda_{q_3}q_4 + \lambda_{q_4}q_3) + \lambda_{\omega_1}\left(\frac{I_3 - I_2}{I_1}\right)\omega_2 + \lambda_{\omega_2}\left(\frac{I_1 - I_3}{I_2}\right)\omega_1
\end{aligned} \qquad (19)$$

Now suppose a general solution to 19 can be obtained; that, is suppose we can find a function, $\mathbf{g}(t; \mathbf{x}_0, \mathbf{x}_f)$ such that

$$\dot{\boldsymbol{\lambda}} = \partial_t\mathbf{g}(t; \mathbf{x}_0, \mathbf{x}_f)$$

holds for any feasible set of boundary conditions. Then, the open-loop solution given by 18 can be transformed to a closed-loop solution by replacing $\mathbf{x}_0$ with $\mathbf{x}$ to yield,

$$u_i = u_{max}sgn(\mathbf{g}_{\omega_i}(t, \mathbf{x}, \mathbf{x}_f)/I_i) \qquad (20)$$

where $\mathbf{g}_{\omega_i}$ is the ω_i component of $\mathbf{g}$. This concept has been used by Pontryagin et al[26] and Bryson and Ho[27] to generate closed-form solutions to a few simple problems. It is clear that the difficulty in obtaining feedback solutions by this approach is the fundamental bottleneck in mathematics in solving nonlinear ordinary differential equations in closed form.

Note that the definition of the *sgn* multifunction (Cf. figure 1) and the ensuing discussions automatically incorporate the special conditions, $t \mapsto \mu_i = 0$, over a nonzero time interval. A complete discussion of these singular conditions are beyond the scope of this paper due to the remarks noted in Appendix II.

IV. Solution Concepts and Methods

Strictly speaking, neither the necessary conditions of Pontryagin nor the sufficiency conditions of Bellman are problem solving techniques.[28] Using either of the conditions to solve the optimal control problem generates theoretical and computational problems. To appreciate this point, suppose we have found the optimal feedback law as given by 17. Now, consider the dynamics,

$$\dot{\omega}_1 = \frac{u_1}{I_1} - \left(\frac{I_3 - I_2}{I_1}\right)\omega_2\omega_3 \tag{21}$$

Then, the closed-loop response is given by the differential inclusion,

$$\dot{\omega}_1 \in \frac{u_{max} sgn(\partial^P_{\omega_1}\varphi(\mathbf{x}, t)/I_1)}{I_1} - \left(\frac{I_3 - I_2}{I_1}\right)\omega_2\omega_3 \tag{22}$$

Because the right-hand side of this differential inclusion is not Lipschitz-continuous, the very definition and notion of a solution is called into question. This point is not merely academic as one needs to ultimately develop numerical methods to solve such equations, and hence, a clear concept of what a solution is needs to be developed. As noted in Ref.[12], this is still an open problem in mathematics because standard solution concepts like the Filippov or Carathéodory solutions are not quite satisfactory. In sharp contrast, a Carathéodory solution is entirely satisfactory for the open-loop response because the discontinuity in the vector field is only with respect to the independent variable; for instance, the open-loop response to 21 is given by,

$$\dot{\omega}_1 = \frac{u_{max} sgn(\lambda_{\omega_i}(t)/I_i)}{I_1} - \left(\frac{I_3 - I_2}{I_1}\right)\omega_2\omega_3 \tag{23}$$

A closed-loop solution can then be obtained, in principle, by way of 20. This approach does not require one to solve a nonsmooth partial differential equation; however, it requires the computation of an optimal solution for generic initial conditions. We accomplish this task by way of PS methods. As noted earlier, because the Pontryagin and Bellman conditions are not problem solving techniques, we use their conditions as verification tools within the context of PS methods. In other words, we take a putative PS solution to the optimal control problem and verify that the solution meets the basic principles of Pontryagin and Bellman. This is how PS methods are currently being used in industrial and military systems,[16–18,29] of which, the most famous of these applications is the flight implementation of the "zero-propellant-maneuver" on the International Space Station.[16,17]

In applying these ideas to the problem at hand, consider a 150 degree "roll maneuver;" i.e. we set $\phi = 150^o$. A candidate PS control solution is shown in figure 2. Before evaluating the optimality of the candidate solution, its feasibility is independently verified along industry-standard principles. That is, a proposed control solution must drive the spacecraft from its known initial state to the desired end state by way of some standard Runge-Kutta (RK) solver. We demonstrate this principle by using the MATLAB® ODE45 routine which uses an explicit one-step Runge-Kutta medium order (4th to 5th order) solver.[30] Propagation results are shown in figure 3 and figure 4. The PS solution is shown in solid lines overlaid with the RK-propagated states shown as '+' marks. The PS solution was obtained by using the MATLAB software package, DIDO.[20]

Having determined that the candidate solution presented in figure 2 is feasible, we next examine the necessary conditions for optimality. If the control solutions shown in figure 2 are optimal, then, according to 18, the functions, $t \mapsto \lambda_{\omega_i}(t)/I_i$ behave as switching functions. A plot of these functions for each axis are shown, in figures 5, 6, and 7. It is clear from these figures that the control solutions satisfy the switching conditions thereby simultaneously validating the satisfaction of the Hamiltonian minimization condition. It is also apparent from these figures that there are no singular arcs. This does not imply that singular arcs do not exist for all such problems. A complete discussion of singular arcs is beyond the scope of this paper; however, we refer to Appendix II of this paper for some preliminary discussions on the optimality conditions for a singular arc. We note that our development automatically incorporates singular arcs by way of the
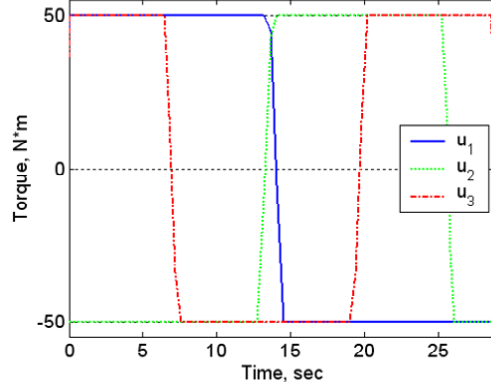
American Institute of Aeronautics and Astronautics

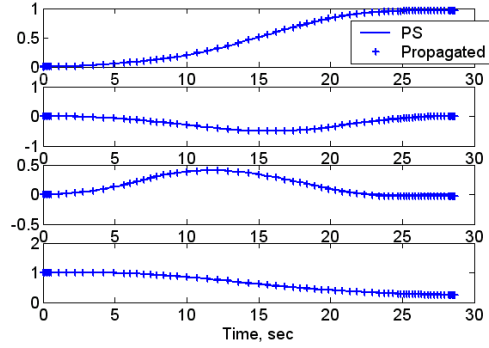**Figure 2. Candidate Solution for the Time-Optimal Problem**

Figure 3. Quaternion PS Solution and its Validation by Propagation.

definition of the *sgn* multifunction. When $\lambda_{\omega_i}(t) = 0$, the *sgn* multifunction takes all values from $[-1, 1]$; see figure 1. Thus, from 18, $u_i(t)$ takes all values from $[-u_{max}, u_{max}]$, i.e. a singular arc. This point once again illustrates how modern nonsmooth analysis completes and unifies classical optimal control theory.

Another verification that is easy to perform is the connection between the lower Hamiltonian and the control Hamiltonian via the Hamiltonian evolution equation,

$$\frac{d\mathcal{H}}{dt} = \frac{\partial H}{\partial t} \tag{24}$$

where the derivative on the left-hand-side of 24 must be interpreted in the nonsmooth sense. It is clear from 7 that $\partial H/\partial t = 0$; hence we have the condition,

$$\mathcal{H}(\boldsymbol{\lambda}(t), \mathbf{x}(t)) = \text{constant}$$

Furthermore, the Hamiltonian value condition requires that,

$$\mathcal{H}(\boldsymbol{\lambda}(t_f), \mathbf{x}(t_f)) = -1$$

for a time-optimal maneuver. Hence, a necessary condition for time optimality is that the lower Hamiltonian must be a constant and numerically equal to -1 over the period of interest. This necessary condition is indeed met with small numeric variations as illustrated in figure 8.
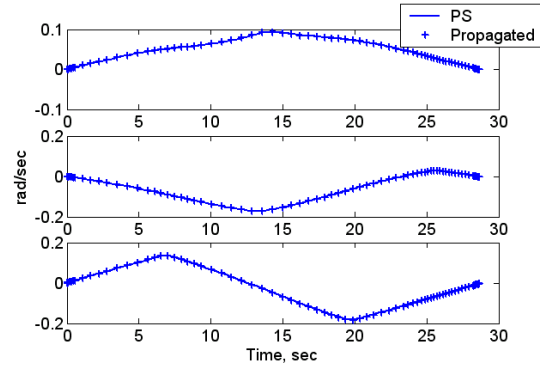
American Institute of Aeronautics and Astronautics

Figure 4. Angular-Rate PS Solution and its Validation by Propagation.
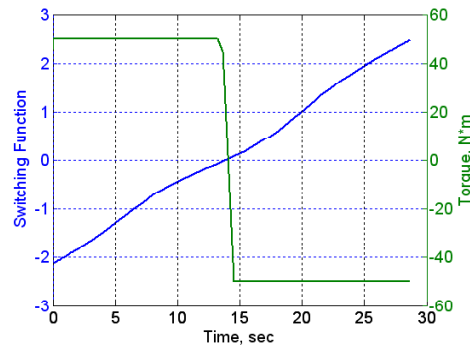

Figure 5.   X-axis Switching Function and Control Solution
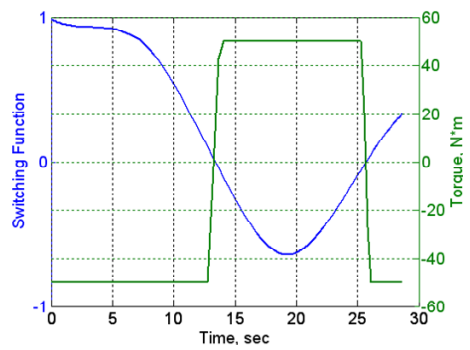

Figure 6.   Y-axis Switching Function and Control Solution

The control Hamiltonian is easy to compute because it is merely a function of the problem data; hence, the necessary conditions for optimality are easy to verify. For the verification of sufficiency conditions, a
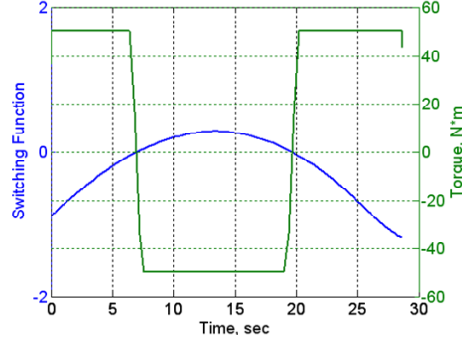
American Institute of Aeronautics and Astronautics

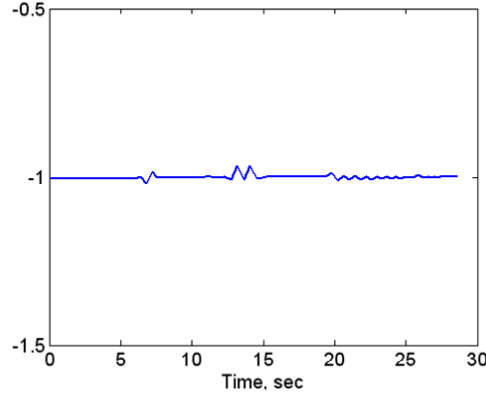**Figure 7. Z-axis Switching Function and Control Solution**

Figure 8. Hamiltonian Validation of the Candidate Time-optimal Maneuver

computation of $\varphi(\mathbf{x}, t)$ is near impossible due to the reasons discussed in Sec. III; however, as discussed in Refs. [31] and [32], it is still possible to use Bellman's Principle of Optimality as another verification tool. That is, according to Bellman's Principle, given an optimal trajectory from a point A to a point B, the trajectory to point B from a point C lying on the optimal trajectory is also optimal. This semi-group property can be directly tested to verify the optimality of a candidate optimal solution by recomputing an optimal solution using an intermediate point on the original trajectory as the new initial condition. For the original open-loop solution to be optimal, the new partial-maneuver solutions must lie exactly on the original complete maneuver trajectory. Figure 9 overlays 3 open-loop optimal trajectories: the original open-loop trajectory derived for the complete maneuver, a second open-loop trajectory derived for the system starting from the state values of the original maneuver at t=10.14 s (dotted lines), and a third open-loop trajectory obtained for the system with initial state values of the original complete maneuver at t=17.96 s (circled markers). The numerically-indistinguishable overlays of the second and third plots demonstrate that the original solution satisfies Bellman's Principle of Optimality at two arbitrarily chosen intermediate points. An arbitrary number of randomly chosen points illustrate the same phenomenon and are not displayed for the purposes of brevity. These plots not only demonstrate the Principle of Optimality, they also lay down the foundations for generating closed loop optimal solutions in a manner that avoids the computational pitfalls associated with solving the proximal HJB equation (see 16). Before discussing this point, we first analyze the "physics" of the time-optimal maneuver.
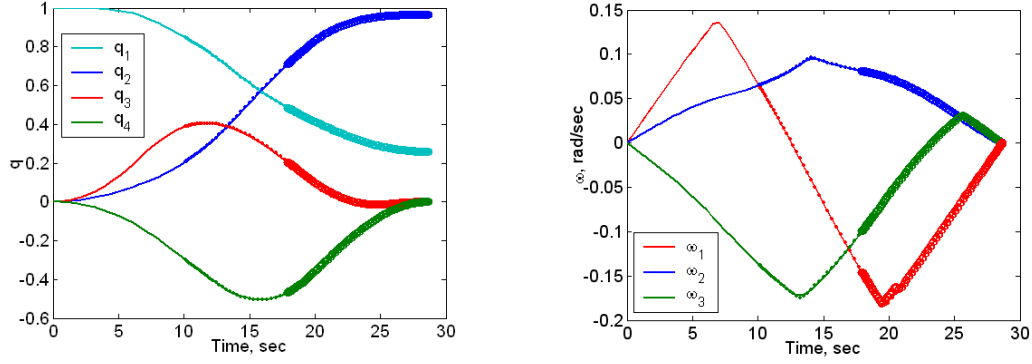
American Institute of Aeronautics and Astronautics

Figure 9. Verifying Bellman's Principle of Optimality

V. Dissecting the Time-Optimal Maneuver

From Fig. 2, it is clear that all three torques are always on for the time-optimal maneuver. Hence, the time-optimal "roll" maneuver is not an eigenaxis maneuver. This point is further illustrated in figure 10 which
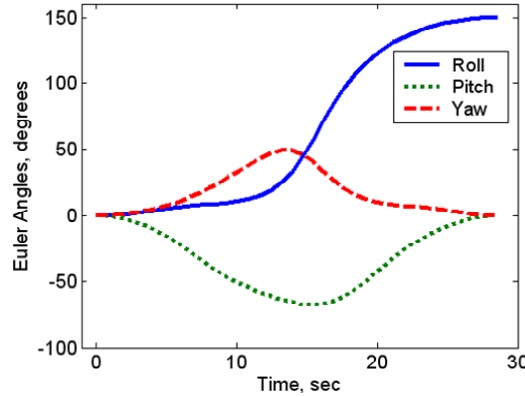

Figure 10. Roll, pith and yaw angles for the time-optimal maneuver.

shows the evolution of the familiar roll, pitch and and yaw angles. This graph shows that the off-eigenaxis deviations are substantial. This point can be explained as follows: The torque capability about any one axis is 50 Nm; however, the net torque capability of the spacecraft per se is $\sqrt{3} \times 50 = 86.6$ Nm; see figure 11 for a 3-D illustration of this concept. Thus, an eigenaxis maneuver utilizes only 50 Nm of torque while the optimal maneuver tends to utilize all 86.6 Nm of torque capability. But because the net maximum torque is not along the eigenaxis (roll), switches are necessary to properly aid the maneuvering. Furthermore, because the inertia ellipsoid is not a sphere (see figure 11), the preferred axis of rotation is the minor axis (yaw for our problem). Thus, what optimal control facilitates, is a balance between the competing interests of preferred rotation about the axis of maximum torque authority, the minor axis, and the eigenaxis.[33] On the basis of this explanation, we can provide back-of-the-envelope formulas for upper and lower bounds on the minimum time maneuver.

For an arbitrary eigenaxis maneuver, the time-optimal maneuver is a bang-bang maneuver with one switch in the middle; see figure 12. Hence, from elementary kinematics, for a rest-to-rest maneuver, we have,
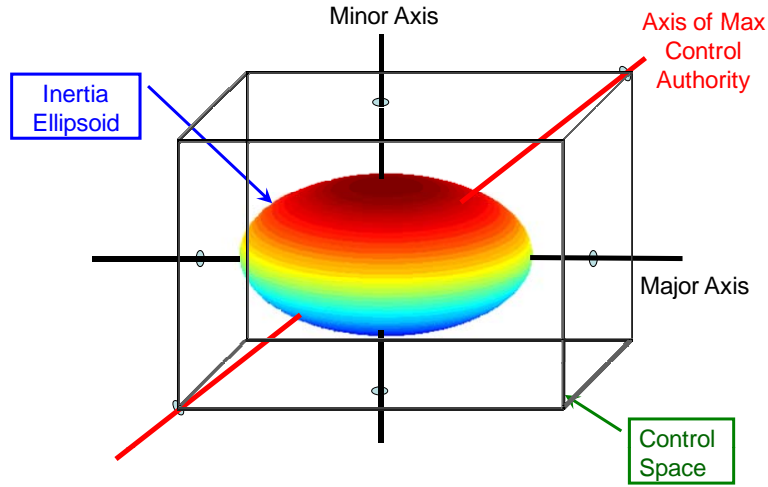
Figure 11. Illustration of the control space and inertia ellipsoid in 3-D

$$t_{min} = \sqrt{\frac{4I\Delta\theta}{T_q}}$$

where T_q is the torque and I is the moment of inertia. Thus, the lower bound of all minimum time maneuvers, t_f^L can be estimated by using the smallest moment of inertia ($2364\ Kg*m^2$) and the largest of the maximum torque capability (86.6Nm). This implies that,

$$t_{min}^L = \sqrt{\frac{4I_{min}\Delta\theta}{\sqrt{3}u_{max}}} = 16.9s$$

Note that this minimum time is truly an estimate for the lower bound and not realizable because the axis of maximum control authority is not the minor axis; see figure 11. By the same procedure, the upper bound of all minimum time maneuvers, t_f^U can be estimated by using the largest moment of inertia ($5621\ Kg*m^2$) and the smallest of the maximum torque capability (50 Nm). This implies that,

$$t_{min}^U = \sqrt{\frac{4I_{max}\Delta\theta}{u_{max}}} = 34.3s$$

Because I_{max} happens to be the inertia about the roll axis, t_{min}^U is, in fact, the cost of the time-optimal fixed-eigenaxis roll maneuver. Comparing this value to the actual time-optimal maneuver of 28.6 seconds it is apparent that nearly 20% of the spacecraft's maneuvering capability is lost by constraining maneuvers about the eigenaxis. A visualization of the time-optimal maneuver is illustrated in figure 13. The green lines are the traces of the tips of the body axes. Thus, the roll axis traces a loop in such a manner that it starts and ends at the same point thereby meeting part of the boundary conditions. In an eigenaxis maneuver, this loop coalesces to a single point because the roll axis does not move, and thus meets the boundary conditions in a more straightforward manner than the time-optimal maneuver. As evident from figure 13, the yaw axis in the time-optimal maneuver does not trace out an arc of a circle as would have been the case for an eigenaxis maneuver, rather it follows a longer and slightly twisted path. In this sense, the time-optimal rigid body maneuver is similar to Bernoulli's famous brachistochrone problem: the shortest and most intuitive path is not the time-optimal path. In the case of the brachistochrone problem, the shortest path is a straight line while the time-optimal path is a cycloid. In the case of the rigid-body problem, the paths can be visualized
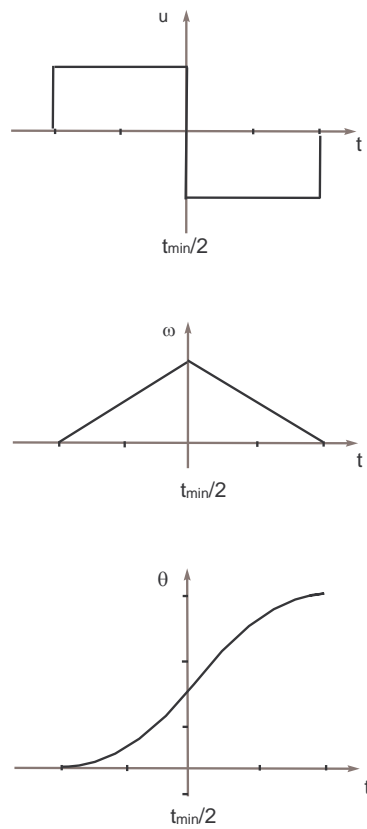
American Institute of Aeronautics and Astronautics

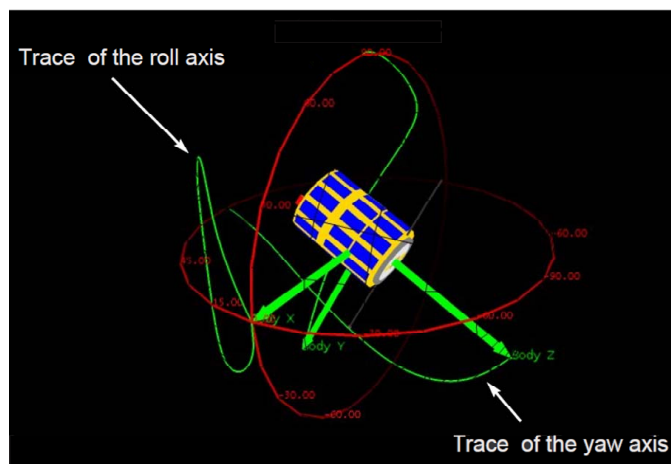**Figure 12. Illustration of a bang-bang eigenaxis maneuver.**

Figure 13. Visualizing the time-optimal maneuver.

in terms of the traces of the axes: the shortest path is an arc of a circle, while the time-optimal path is a different, longer path that does not have a closed-form expression.

American Institute of Aeronautics and Astronautics

VI. Illustrating the Possibility of Exploiting Uncertainties

The direct application of Bellman's Principle as illustrated in figure 9 may be viewed as a three-sample closed-loop solution. Over each sample, the solution is a valid Carathéodory solution. The full solution is a semidiscrete semianalog representation of a closed-loop solution.[12] As the number of samples increase, and, in principle, tend to infinity, the limiting solution is a solution to the proximal HJB equation. This solution is the limit of the sequence of Carathéodory-π solutions with the diameter of π tending to zero. Mathematical details on the existence of the limit are discussed by Clarke.[13, 15] A practical implementation of this concept does not require $diam(\pi) \to 0$, but that it be sufficiently small. This sufficiency condition is related to the Lipschitz constant of the dynamical system.[12] Thus, the Carathéodory-π solution concept allows us to generate practical closed-loop solutions to dynamical systems without directly solving the proximal HJB equation. This concept is similar in principle to computing open-loop solutions without directly solving for the adjoint equations as illustrated in Sec. IV. Similar to the verification of Pontryagin's Principle for open-loop solutions, we first verify Bellman's Principle for closed-loop solutions.

A. Closed-Loop Control for System with Known Parameters

The closed-loop response for the system with known parameters is shown in figure 14. It is clear that
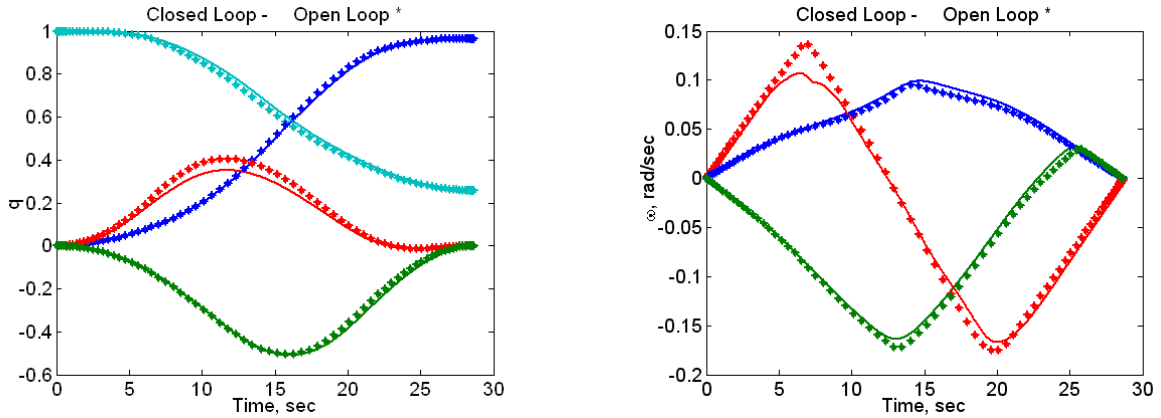

Figure 14. Open-Loop vs. Closed-Loop State Trajectories for the System with Known Parameters

the open-loop and closed-loop responses are identical (within numerical tolerances) as expected. The small differences in the plots are due the combination of non-zero errors in the RK propagation and the finiteness of the diameter of π. For practical applications, we regard these inevitable numerical sources of errors as part of sensor measurement errors, uncertainty in system parameters, and possibly exogenous disturbance torques that are never zero in any real system.[12] In any event, it is clear that the closed-loop response matches the optimal open-loop solution.

The control trajectories corresponding to figure 14 are shown in figure 15. A key desirable feature inherent in such control algorithms is the fact that it is "gain-free" and does not require the control designer to select or tune any controller gains; see Ref. [12] for further details.

B. Closed-Loop Control with Parameter Uncertainties

For spacecraft attitude control, one of the primary reasons for feedback is the uncertainty in the moments of inertia. Motivated by this argument, we suppose that the rigid body's real moments of inertia, I_1, I_2, and I_3 are off from the estimate (see Table 1) by 28%, 15% and 12% respectively. Then, the closed-loop response is as indicated in figure 16. What is interesting about this solution is that the closed-loop maneuver time is 27 seconds, or about 1.6 seconds faster than the open-loop minimum time! At first glance, this appears to be incorrect, particularly since the open- and closed-loop solutions match (see figure 14) when the parameters are known. In order to appreciate the point that it is indeed possible for the closed-loop response of a spacecraft
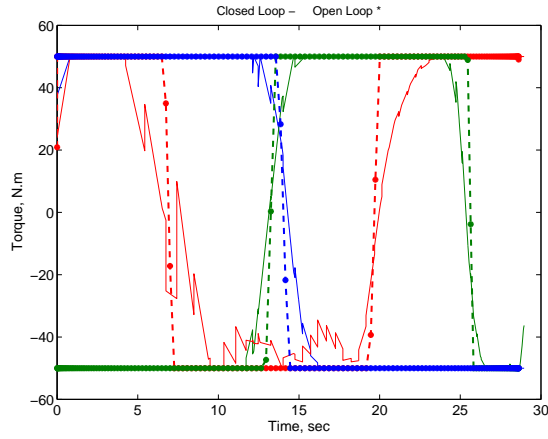
Figure 15. Open-Loop vs. Closed-Loop Control Trajectories for the System with Known Parameters
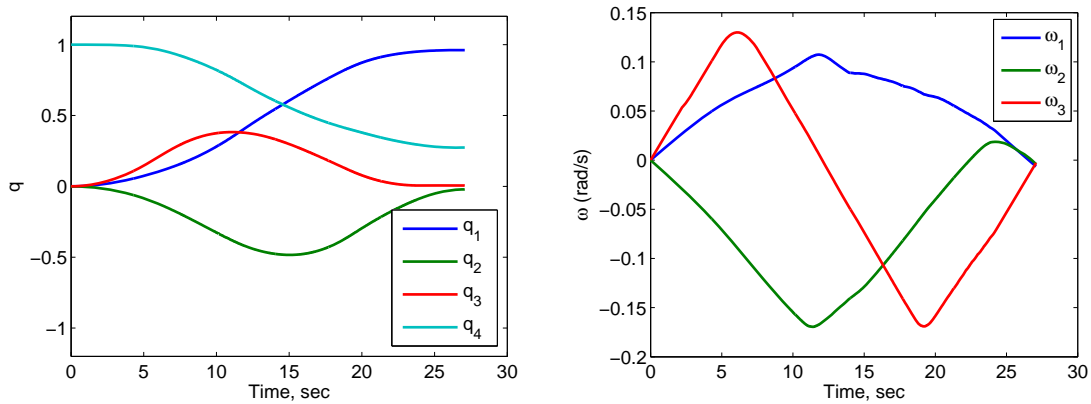

Figure 16. Closed-Loop State Trajectories for Parameter Uncertainties That Aid Optimality

to be better than the open-loop optimal solution, we need to keep in mind that the plant parameters may be unknown in such a manner that they may actually assist in improving the performance of the closed-loop system when optimal control theory is used to construct the feedback control. To further illustrate this point, the open-loop response of the spacecraft was recomputed using the true values of I_1, I_2, and I_3. The cost of this minimum-time open-loop solution is 25.6 seconds. Thus, the closed-loop response is not faster than the true minimum-time solution, rather, it is faster than the minimum-time solution of the spacecraft model that is based on the estimates of the system parameters. For the purpose of brevity, the open-loop response of the spacecraft is not shown; however, for the purpose of completeness, the closed-loop control trajectory is shown in figure 17.

The preceding analysis shows that when optimal control theory is used to construct feedback solutions, effects of parameter uncertainties are not necessarily negated; rather, if the parameter uncertainties are lined up in such a manner that they may add an improvement to the optimal open-loop solution, then the optimal closed-loop solution will indeed exploit this feature. *This is in sharp contrast to traditional feedback control systems which are designed to negate the effect of parameter uncertainties whether or not they may aid or assist the performance of the plant.* Of course, the optimal feedback solution will naturally negate the effect or parameter uncertainties should these parameters be lined up in a manner that hinders the performance of the closed-loop system. This feature is illustrated in figure 18 which shows the closed-loop response of the spacecraft when the inertia values are %2 less, %7.8 more, and %8.5 more than its estimated values (see Table 1) along the x-, y- and z-directions respectively.
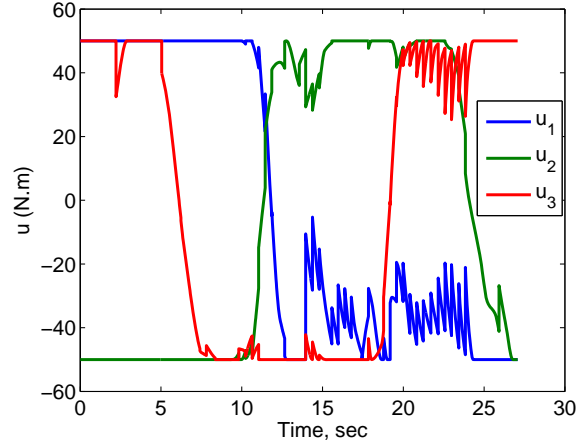
American Institute of Aeronautics and Astronautics

Figure 17. Closed-Loop Control Trajectories Corresponding to Fig. 16.
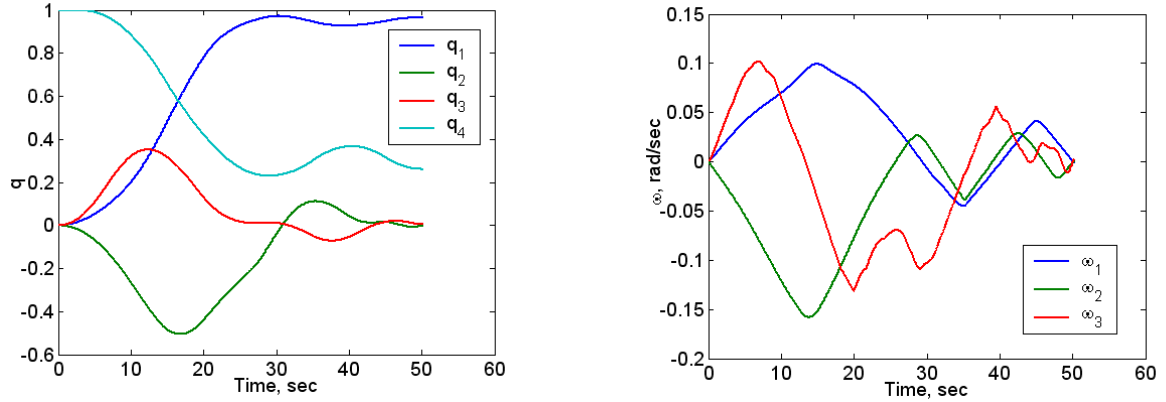

Figure 18. Closed-Loop State Trajectories for Parameter Uncertainties that Hinder Optimality

VII. Conclusions

The problem of reorienting a rigid body in a time-optimal manner poses fundamental challenges in both theory and computation. Advances in optimal control theory over the last decade have shown that the theoretical problems can be overcome by expanding the notion of differentiability to nondifferentiable functions by way of nonsmooth calculus. Computing optimal controls using either the necessary or the sufficient conditions leads to near insurmountable challenges known as the twin curses of complexity and dimensionality. In this paper we have shown that the time-optimal controls for a rigid body can indeed be computed by way of pseudospectral methods. In pseudospectral methods, the neccessary conditions are not directly used for computation; rather, the necessary conditions are used strictly as necessary conditions; i.e. applied for verifying the optimality of a candidate optimal control by way of Pontryagin's Principle. Another verification test is conducted by a direct application of Bellman's Principle of Optimality. The notion of a Carathéodory-π solution completes a trifecta of principles for open- and closed-loop control. Application of these principles to analyzing the time-optimal reorientation of a rigid body reveals that the optimal torque is engaged in exploiting and balancing between the competing interests of the axis of maximum torque authority, the minor axis and the eigenaxis. This behavior of the optimal control implies that in closed-loop applications, it is quite possible for a rigid body with uncertain parameters to exhibit performances that are apparently better than optimal. This apparent contradiction that arises in experimentation can be

explained by comparing the closed-loop solution to an open-loop solution under the assumption of known parameters. In this case, the closed-loop result is at best equal in performance to the open-loop solution; thus, the apparent gains in closed-loop performance is merely a result of the uncertainties in parameters assisting the performance of the closed-loop solution. Thus, optimal feedback control does not necessarily negate the effect of parameter uncertainties in all situations. It turns out that optimal feedback control has inherent intelligence in exploiting or negating the effect of uncertainties without any *a priori* information on the nature of these uncertainties.

VIII.   Appendix I: Carathéodory Concepts

A.   Carathéodory Solution[14, 26]

An initial value (Cauchy) problem,

$$\dot{x} = g(x,t), \quad x(t_0) = x^0$$

where $g(x,t)$ is a time-varying vector field, $g : \mathbb{R}^{N_x} \times \mathbb{R} \to \mathbb{R}^{N_x}$, is said to have a Carathéodory solution if there exits an absolutely continuous function, $x^*(\cdot) : R \supset [t_0, t_f] \to \mathbb{R}^{N_x}$, such that

$$\dot{x}^*(t) = g(x^*(t), t) \; for \; a.a. \; t \in [t_0, t_f] \quad and \quad x^*(t_0) = x^0$$

When $g(x,t)$ is nonsmooth, the Carathéodory solution concept is unsatisfactory from the point of view of existence and uniqueness.[34] These problems are overcome by the notion of a Carathéodory-π solution.

B.   Cauchy Problem and Feedback Control[12, 13]

The initial value problem,

$$\dot{x} = g(x,t), \quad x(t_0) = x^0$$

is equivalent to the controlled differential equation,

$$\dot{x} = u, \quad x(t_0) = x^0$$

with feedback control,

$$u = g(x,t)$$

C.   A Carathéodory-π Trajectory[12, 15]

Let $\pi = \{t_i\}_{i \geq 0}$ be a partition of the time interval, $[0, \infty)$, with $t_i \to \infty$ as $i \to \infty$. The quantity,

$$diam(\pi) := \sup_{i \geq 0}(t_{i+1} - t_i)$$

is called the diameter of π. Given an initial value problem,

$$\dot{x} = g(x,t), \quad x(t_0) = x^0$$

a Carathéodory-π trajectory, $x(\cdot)$, is defined as follows: From t_0 to t_1, generate a control trajectory,

$$u(t) = g(x^0, t), \quad x(t_0) = x^0, \quad t_0 \leq t \leq t_1 \tag{25}$$

to the controlled differential equation,

$$\dot{x} = u(t), \quad x(t_0) = x^0 \tag{26}$$

A Carathéodory solution solution exists for (26) because $t \mapsto u$ has discontinuities at most in t, the independent variable. At $t = t_1$, we set $x^1 = x(t_1)$ and restart the system with $u(t) = g(x^1, t)$,

$$\dot{x}(t) = u(t), \quad x(t_1) = x^1, \quad t_1 \leq t \leq t_2$$

Continuing in this manner, the Carathéodory segments are glued together to form a Carathéodory-π trajectory. Under the concept of a Carathéodory-π trajectory, it is possible to rigorously prove a rich number of theorems[13, 15] that have practical consequences. These theorems directly connect the "epsilons and deltas" of abstract mathematics to practical digital computer implementations of optimal control.[12, 13, 28]

IX.   Appendix II: On Singular Arcs

A.   Degree of a Singular Arc[35]

Let

$$\dot{x} = f(x, u), \qquad u \in \mathbb{U} \subseteq \mathbb{R}^{N_u}$$

be a controlled nonlinear differential system where $f(x, u)$ is a controlled vector field, $f : \mathbb{R}^{N_x} \times \mathbb{R}^{N_u} \to \mathbb{R}^{N_x}$. Let (t_1, t_2) be an open nonzero interval. A control $u_i \in \mathbb{R}, i = 1, \dots, N_u$, is said to be of degree m_i on $[t_1, t_2]$ if m_i is the smallest integer such that for $t \in (t_1, t_2)$, the adjoint covector $\lambda(t)$ satisfies,

$$\frac{d^k}{dt^k} \frac{\partial}{\partial u_i} H(\lambda(t), x(t), u(t)) = 0$$

for $k = 0, \dots, \infty$, and

$$\frac{\partial}{\partial u_i} \frac{d^{m_i}}{dt^{m_i}} \frac{\partial}{\partial u_i} H(\lambda(t), x(t), u(t)) \neq 0$$

If $m_i < \infty$, then m_i is even; see Ref. [35].

Applying these definitions for the rigid-body problem, we have,

$$\frac{d}{dt} \frac{\partial H}{\partial u_j} = \frac{\dot{\lambda}_{\omega_j}}{I_j} \qquad j = 1, 2, 3$$

This implies the following set of conditions (corresponding to $k = 1$) for the optimality of a singular arc,

$$\frac{d}{dt} \frac{\partial H}{\partial u_1} = \frac{1}{2I_1} \left(-\lambda_{q_1} q_4 - \lambda_{q_2} q_3 + \lambda_{q_3} q_2 + \lambda_{q_4} q_1 \right) + \lambda_{\omega_2} \left(\frac{I_1 - I_3}{I_2 I_1} \right) \omega_3 + \lambda_{\omega_3} \left(\frac{I_2 - I_1}{I_3 I_1} \right) \omega_2 = 0$$

$$\frac{d}{dt} \frac{\partial H}{\partial u_2} = \frac{1}{2I_2} \left(\lambda_{q_1} q_3 - \lambda_{q_2} q_4 - \lambda_{q_3} q_1 + \lambda_{q_4} q_2 \right) + \lambda_{\omega_1} \left(\frac{I_3 - I_2}{I_1 I_2} \right) \omega_3 + \lambda_{\omega_3} \left(\frac{I_2 - I_1}{I_3 I_2} \right) \omega_1 = 0$$

$$\frac{d}{dt} \frac{\partial H}{\partial u_3} = \frac{1}{2I_3} \left(-\lambda_{q_1} q_2 + \lambda_{q_2} q_1 - \lambda_{q_3} q_4 + \lambda_{q_4} q_3 \right) + \lambda_{\omega_1} \left(\frac{I_3 - I_2}{I_1 I_3} \right) \omega_2 + \lambda_{\omega_2} \left(\frac{I_1 - I_3}{I_2 I_3} \right) \omega_1 = 0$$

Differentiating these equations again, we get,

$$\frac{d^2}{dt^2} \frac{\partial H}{\partial u_1} = -\frac{\lambda_{\omega_2} (I_3 - I_1) u_3}{I_1 I_2 I_3} - \frac{\lambda_{\omega_3} (I_1 - I_2) u_2}{I_1 I_2 I_3} - \frac{q_4}{4I_1} \left(\lambda_{q_2} \omega_3 - \lambda_{q_3} \omega_2 + \lambda_{q_4} \omega_1 \right)$$

$$- \frac{\lambda_{q_1}}{4I_1} \left(-\omega_1 q_1 - \omega_2 q_2 - \omega_3 q_3 \right) - \frac{q_3}{4I_1} \left(-\lambda_{q_1} \omega_3 + \lambda_{q_3} \omega_1 + \lambda_{q_4} \omega_2 \right)$$

$$- \frac{\lambda_{q_2}}{4I_1} \left(-\omega_1 q_2 + \omega_2 q_1 + \omega_3 q_4 \right) + \frac{q_2}{4I_1} \left(\lambda_{q_1} \omega_2 - \lambda_{q_2} \omega_1 + \lambda_{q_4} \omega_3 \right)$$

$$+ \frac{\lambda_{q_3}}{4I_1} \left(\omega_1 q_3 + \omega_2 q_4 - \omega_3 q_1 \right) + \frac{q_1}{4I_1} \left(-\lambda_{q_1} \omega_1 - \lambda_{q_2} \omega_2 - \lambda_{q_3} \omega_3 \right)$$

$$+ \frac{\lambda_{q_4}}{4I_1} \left(\omega_1 q_4 - \omega_2 q_3 + \omega_3 q_2 \right)$$

$$- \frac{(I_3 - I_1) \omega_3}{I_1 I_2} \left[\frac{1}{2} \left(\lambda_{q_1} q_3 - \lambda_{q_2} q_4 - \lambda_{q_3} q_1 + \lambda_{q_4} q_2 \right) - \frac{\lambda_{\omega_1} (I_2 - I_3) \omega_3}{I_1} - \frac{\lambda_{\omega_3} (I_1 - I_2) \omega_1}{I_3} \right]$$

$$- \frac{\lambda_{\omega_2} (I_3 - I_1) (I_1 - I_2) \omega_1 \omega_2}{I_1 I_2 I_3}$$

$$- \frac{(I_1 - I_2) \omega_2}{I_1 I_3} \left[\frac{1}{2} \left(-\lambda_{q_1} q_2 + \lambda_{q_2} q_1 - \lambda_{q_3} q_4 + \lambda_{q_4} q_3 \right) - \frac{\lambda_{\omega_1} (I_2 - I_3) \omega_2}{I_1} - \frac{\lambda_{\omega_2} (I_3 - I_1) \omega_1}{I_2} \right]$$

$$- \frac{\lambda_{\omega_3} (I_1 - I_2) (I_3 - I_1) \omega_1 \omega_3}{I_1 I_2 I_3}$$

$$\frac{d^2}{dt^2}\frac{\partial H}{\partial u_2} = -\frac{\lambda_{\omega_1}(I_2 - I_3)u_3}{I_1 I_2 I_3} - \frac{\lambda_{\omega_3}(I_1 - I_2)u_1}{I_1 I_2 I_3} + \frac{q_3}{4I_2}\left(\lambda_{q_2}\omega_3 - \lambda_{q_3}\omega_2 + \lambda_{q_4}\omega_1\right)$$

$$+ \frac{\lambda_{q_1}}{4I_2}\left(-\omega_1 q_2 + \omega_2 q_1 + \omega_3 q_4\right) - \frac{q_4}{4I_2}\left(-\lambda_{q_1}\omega_3 + \lambda_{q_3}\omega_1 + \lambda_{q_4}\omega_2\right)$$

$$- \frac{\lambda_{q_2}}{4I_2}\left(-\omega_1 q_1 - \omega_2 q_2 - \omega_3 q_3\right) - \frac{q_1}{4I_2}\left(\lambda_{q_1}\omega_2 - \lambda_{q_2}\omega_1 + \lambda_{q_4}\omega_3\right)$$

$$- \frac{\lambda_{q_3}}{4I_2}\left(\omega_1 q_4 - \omega_2 q_3 + \omega_3 q_2\right) + \frac{q_2}{4I_2}\left(-\lambda_{q_1}\omega_1 - \lambda_{q_2}\omega_2 - \lambda_{q_3}\omega_3\right)$$

$$+ \frac{\lambda_{q_4}}{4I_2}\left(\omega_1 q_3 + \omega_2 q_4 - \omega_3 q_1\right)$$

$$- \frac{(I_2 - I_3)\omega_3}{I_1 I_2}\left[\frac{1}{2}\left(-\lambda_{q_1}q_4 - \lambda_{q_2}q_3 + \lambda_{q_3}q_2 + \lambda_{q_4}q_1\right) - \frac{\lambda_{\omega_2}(I_3 - I_1)\omega_3}{I_2} - \frac{\lambda_{\omega_3}(I_1 - I_2)\omega_2}{I_3}\right]$$

$$- \frac{\lambda_{\omega_1}(I_2 - I_3)(I_1 - I_2)\omega_1\omega_2}{I_1 I_2 I_3}$$

$$- \frac{(I_1 - I_2)\omega_1}{I_2 I_3}\left[\frac{1}{2}\left(-\lambda_{q_1}q_2 + \lambda_{q_2}q_1 - \lambda_{q_3}q_4 + \lambda_{q_4}q_3\right) - \frac{\lambda_{\omega_1}(I_2 - I_3)\omega_2}{I_1} - \frac{\lambda_{\omega_2}(I_3 - I_1)\omega_1}{I_2}\right]$$

$$- \frac{\lambda_{\omega_3}(I_1 - I_2)(I_2 - I_3)\omega_2\omega_3}{I_1 I_2 I_3}$$

$$\frac{d^2}{dt^2}\frac{\partial H}{\partial u_3} = -\frac{\lambda_{\omega_2}(I_3 - I_1)u_1}{I_1 I_2 I_3} - \frac{\lambda_{\omega_1}(I_2 - I_3)u_2}{I_1 I_2 I_3} - \frac{q_2}{4I_3}\left(\lambda_{q_2}\omega_3 - \lambda_{q_3}\omega_2 + \lambda_{q_4}\omega_1\right)$$

$$- \frac{\lambda_{q_1}}{4I_3}\left(\omega_1 q_3 + \omega_2 q_4 - \omega_3 q_1\right) + \frac{q_1}{4I_3}\left(-\lambda_{q_1}\omega_3 + \lambda_{q_3}\omega_1 + \lambda_{q_4}\omega_2\right)$$

$$+ \frac{\lambda_{q_2}}{4I_3}\left(\omega_1 q_4 - \omega_2 q_3 + \omega_3 q_2\right) - \frac{q_4}{4I_3}\left(\lambda_{q_1}\omega_2 - \lambda_{q_2}\omega_1 + \lambda_{q_4}\omega_3\right)$$

$$- \frac{\lambda_{q_3}}{4I_3}\left(-\omega_1 q_1 - \omega_2 q_2 - \omega_3 q_3\right) + \frac{q_3}{4I_3}\left(-\lambda_{q_1}\omega_1 - \lambda_{q_2}\omega_2 - \lambda_{q_3}\omega_3\right)$$

$$+ \frac{\lambda_{q_4}}{4I_3}\left(-\omega_1 q_2 + \omega_2 q_1 + \omega_3 q_4\right)$$

$$- \frac{(I_2 - I_3)\omega_2}{I_1 I_3}\left[\frac{1}{2}\left(-\lambda_{q_1}q_4 - \lambda_{q_2}q_3 + \lambda_{q_3}q_2 + \lambda_{q_4}q_1\right) - \frac{\lambda_{\omega_2}(I_3 - I_1)\omega_3}{I_2} - \frac{\lambda_{\omega_3}(I_1 - I_2)\omega_2}{I_3}\right]$$

$$- \frac{\lambda_{\omega_1}(I_2 - I_3)(I_3 - I_1)\omega_1\omega_3}{I_1 I_2 I_3}$$

$$- \frac{(I_3 - I_1)\omega_1}{I_2 I_3}\left[\frac{1}{2}\left(\lambda_{q_1}q_3 - \lambda_{q_2}q_4 - \lambda_{q_3}q_1 + \lambda_{q_4}q_2\right) - \frac{\lambda_{\omega_1}(I_2 - I_3)\omega_3}{I_1} - \frac{\lambda_{\omega_3}(I_1 - I_2)\omega_1}{I_3}\right]$$

$$- \frac{\lambda_{\omega_2}(I_3 - I_1)(I_2 - I_3)\omega_2\omega_3}{I_1 I_2 I_3}$$

It is now clear that

$$\frac{\partial}{\partial u_i}\frac{d^2}{dt^2}\frac{\partial}{\partial u_i}H(\lambda(t), x(t), u(t)) = 0 \qquad i = 1, 2, 3$$

Thus, the degree of any singular control for the rigid body problem is at least four. Note that this conclusion remains valid for any endpoint cost function, for any set of boundary conditions and for any set of inertias.

B.   Krener's Theorem[35]

Suppose $u(t) \in$ interior $\mathbb{U}$ and each u_i is singular of degree m_i over (t_1, t_2). If $u(t)$ is minimal, then,

$$\frac{\partial}{\partial u_i}\frac{d^k}{dt^k}\frac{\partial}{\partial u_j}H(\lambda(t), x(t), u(t)) = 0$$

for $k = 0, \ldots, (m_i + m_j - 2)/2,\ 1 \le i, j \le N_u$.

C. Application of Krener's Theorem

Because the degree of any singular control for the rigid body problem is at least four, it is clear that we can apply Krener's theorem for at least $k = 0, 1, 2, 3$ corresponding to the case when all three controls are singular. Applying this result for $k = 2$, we get the following conditions,

$$\lambda_{\omega_2}(I_3 - I_1) = 0 \tag{27}$$
$$\lambda_{\omega_3}(I_1 - I_2) = 0 \tag{28}$$
$$\lambda_{\omega_1}(I_2 - I_3) = 0 \tag{29}$$

These conditions yield no new information for the tri-axisymmetric case, $I_1 = I_2 = I_3$, considered first by Bilimoria and Wie.[1] When the body is asymmetric, i.e. $I_1 \neq I_2 \neq I_3$, then we get,

$$\lambda_{\omega_j} = 0 \qquad j = 1, 2, 3$$

Thus, additional analysis is necessary to fully examine the optimality of possible singular arcs.

References

[1]Bilimoria, K.D., and Wie, B., "Time-Optimal Three-Axis Reorientation of Rigid Spacecraft," *Journal of Guidance, Control, and Dynamics*, Vol. 16, No. 3, 1993, pp. 446-452.

[2]Shen, H. and Tsiotras, P., "Time-Optimal Control of Axisymmetric Rigid Spacecraft Using Two Controls," *Journal of Guidance, Control, and Dynamics*, Vol. 22, No. 5, 1999, pp. 682-694.

[3]Tsiotras, P., and Longuski, J.M., "A New Parameterization of the Attitude Kinematics," *The Journal of the Astronautical Sciences*, Vol. 43, No. 3., 1995, pp. 243-263.

[4]Proulx, R. and Ross, I. M., "Time-Optimal Reorientation of Asymmetric Rigid Bodies," *AAS/AIAA Astrodynamics Specialist Conference*, Quebec City, Canada, 30 July - 2 August, 2001.

[5]Fahroo, F., Ross, I.M., "Costate Estimation by a Legendre Pseudospectral Method," *Journal of Guidance, Control, and Dynamics*, Vol. 24, No. 2, 2001, pp. 270-277.

[6]Elnagar, J., Kazemi, M.A. and Razzaghi, M., " The Pseudospectral Legendre Method for Discretizing Optimal Control Problems," *IEEE Transactions on Automatic Control*, Vol. 40, No. 10, 1995, pp. 1793-1796.

[7]Ross, I. M., and Fahroo, F., "Legendre Pseudospectral Approximations of Optimal Control Problems," *Lecture Notes in Control and Information Sciences*, Vol. 295, Springer-Verlag, New York, 2003.

[8]Kang, W., Ross, I. M., and Gong, Q., "Pseudospectral Optimal Control and Its Convergence Theorems," *Analysis and Design of Nonlinear Systems*, Springer, Berlin, November 2007, pp. 109-124.

[9]Fleming, A., "Real-time Optimal Slew Maneuver Design and Control." Astronautical Engineer's Thesis, US Naval Post-graduate School, 2004.

[10]Fleming, A., Sekhavat, P. and Ross, I. M., "Minimum-Time Reorientation of a Rigid Body," AIAA Paper No. 2008-7012.

[11]Fleming, A. and Ross, I. M., "Optimal Control of Spinning Axisymmetric Spacecraft: A Pseudospectral Approach," AIAA Paper No. 2008-7164.

[12]Ross, I. M., Sekhavat, P., Fleming, A. and Gong, Q., Optimal feedback control: foundations, examples and experimental results for a new approach, *Journal of Guidance, Control and Dynamics*, Vol. 31, No. 2, pp. 307-321, 2008.

[13]Clarke, F., "Lyapunov functions and feedback in nonlinear control," *Optimal Control, Stabilization and Nonsmooth Analysis*, M.S. de Queiroz, M. Malisoff, P. Wolenski (Eds.), Lecture Notes in Control and Information Sciences Vol. 301, pp. 267-282, Springer-Verlag, 2004.

[14]Biles, D. C. and Binding, P. A., "On Carathéodory's Conditions for the Initial Value Problem," *Proceedings of the American Mathematical Society*, Volume 125, Number 5, May 1997, Pages 1371-1376.

[15]Clarke, F. H., Ledyaev, Y. S., Stern, R. J., and Wolenski, P. R., *Nonsmooth Analysis and Control Theory*, Springer-Verlag, New York, NY, 1998. Chapter 4.

[16]Bedrossian, N., Bhatt, S., Lammers, M., Nguyen, L., and Zhang, Y., First ever flight demonstration of zero propellant maneuver attitude control concept, *AIAA Guidance, Navigation and Control Conference*, 2007. AIAA-2007-6734.

[17]Kang, W. and Bedrossian, N., Pseudospectral optimal control theory makes debut flight, *SIAM News, Volume 40, Number 7, September 2007.*

[18]Gong, Q., Kang, W., Bedrossian, N., Fahroo, F., Sekhavat, P., Bollino, K., "Pseudospectral Optimal Control for Military and Industrial Applications," *Proceedings of the 46th IEEE Conference on Decision and Control*, New Orleans, LA, pp. 4128-4142, December 2007.

[19]Paris, S. W. and Hargraves, C. R., *OTIS 3.0 Manual*, Boeing Space and Defense Group, Seattle, WA, 1996.

[20]Ross, I. M., "A Beginner's Guide to DIDO: A MATLAB Application Package for Solving Optimal Control Problems," *Elissar Technical Report TR-711,*, http://www.elissar.biz, 2007.

[21]Sidi, M.J., *Spacecraft Dynamics and Control*, Cambridge University Press, New York, NY, 1997. Chapter 4.

[22]Vinter, R. B., *Optimal Control*, Birkhäuser, Boston, MA, 2000. Chapters 1, 6, 9, 11 and 12.

[23]Bazaraa, M. S., Sherali, H. D., and Shetty, C. M., *Nonlinear Programming: Theory and Algorithms*, John Wiley and Sons, Inc., 2006.

[24]McEneaney, W. M., "A curse-of-dimensionality-free numerical method for solution of certain HJB PDEs," *SIAM Journal on Control and Optimization*, Vol. 46 , No. 4, pp. 1239-1276, 2007.

[25]McEneaney, W. M., "Max-plus summation of Fenchel-transformed semigroups for solution of nonlinear Bellman equations," *Systems & Control Letters*, Vol. 56, No. 4, pp. 255–264, 2007.

[26]Pontryagin, L.S., Boltyanskii, V.G., Gramkrelidze, R.V. and Mishchenko, E.F., *The Mathematical Theory of Optimal Processes*, John Wiley and Sons, Inc., New York, NY, 1962. Chapter 1.

[27]Bryson, A. E. and Ho, Y., *Applied Optimal Control*, Taylor & Francis Publishing, New York, NY, 1975. Chapter 5.

[28]Ross, I. M., "A Roadmap for Optimal Control: The Right Way to Commute," *Annals of the New York Academy of Sciences*, Vol. 1065, New York, N.Y., January 2006.

[29]Sekhavat, P., Fleming, A., and Ross, I.M., "Time-Optimal Nonlinear Feedback Control for the NPSAT1 Spacecraft," *Proceedings of the 2005 IEEE/ASME International Conference on Advanced Intelligent Mechatronics*, July 23-28, 2005, Monterey, CA.

[30]Hanselman, D., and Littlefield, B., *Mastering MATLAB® 6*, Prentice Hall, Upper Saddle River, NJ, 2001. Chapter 8.

[31]Ross, I. M., Gong, Q. and Sekhavat, P., "Low-Thrust, High-Accuracy Trajectory Optimization," *Journal of Guidance, Control and Dynamics*, Vol. 30, No. 4, pp. 921-933, 2007.

[32]Ross, I. M. and Gong, Q. *Emerging Principles in Fast Trajectory Optimization* Elissar Publications, Monterey, CA 2008.

[33]Ross, I. M., "Space Trajectory Optimization and L^1-Optimal Control Problems," *Modern Astrodynamics*, Elsevier, St. Louis, MO, September 2006.

[34]Filippov, A. F., *Differential Equations with Discontinuous Right-Hand Side*, D. Reidel, Boston, 1989. Chapter 1 and 2.

[35]Krener, A. J., "The High Order Maximal Principle and its Applications to Singular Extremals," *SIAM Journal of Control and Optimization*, Vol. 15, No. 2, pp. 256-293, 1977.